First published in:

Available online at www.sciencedirect.com
ScienceDirect

Applied Catalysis A: General 318 (2007) 160–169

APPLIED CATALYSIS A: GENERAL

www.elsevier.com/locate/apcata

Catalytic vapour phase epoxidation of propene with nitrous oxide as an oxidant
I. Reaction network and product distribution

Thomas Thömmes, Sebastian Zürcher, Andrea Wix, Andreas Reitzmann *, Bettina Kraushaar-Czarnetzki

Institute of Chemical Process Engineering, University of Karlsruhe (TH), Kaiserstr. 12, 76185 Karlsruhe, Germany

Received 16 August 2006; received in revised form 27 October 2006; accepted 31 October 2006
Available online 15 December 2006

Abstract

The vapour phase epoxidation of propene with nitrous oxide (N_2O) was experimentally investigated in a fixed bed reactor using a $CsO_x/FeO_y/SiO_2$ catalyst in a broad range of residence times. A complex reaction network was derived from the trends of product selectivities as function of the conversion. For the determination of the reaction paths, not only propene but also its oxidation products, propylene oxide (PO) and propionaldehyde (PA), were used as reactants. The selectivity to PO was found to be limited due to fast side reactions, like PO isomerisation reactions and, in particular, the formation of higher molecular weight products (HMP) mainly present as carbonaceous deposits (coke) on the catalyst. The amount of HMP and coke was quantified through several methods and both were identified as the major byproducts. Although PO is formed with more than 60% selectivity among the directly identified vapour phase products, the maximum selectivity is only about 30% when taking the HMP into account.

Keywords: Reaction engineering; Partial oxidation; Propylene oxide; Propionaldehyde; Iron oxide; Silica gel; Reaction network; Carbon balance; Coke

1. Introduction

Propylene oxide (PO) is an important intermediate for the chemical industry with a worldwide production capacity of more than 5×10^6 t/a [1]. However, PO production technology is still dominated by disadvantageous, liquid phase processes containing multiple reaction steps, namely the chlorhydrine process and several peroxidation routes [1–3]. Particularly in the last 10 years, different approaches led to progress concerning a direct epoxidation of propene. In the liquid phase, heterogeneously and homogeneously catalysed propene epoxidation with ex situ and in situ produced hydrogen peroxide as oxidant seem to be the most developed [4,5]. High prices for H_2O_2, however, still put the profitability of these processes under debate [3]. Furthermore, a high amount of organic solvent reacting with both the feed and the products, catalyst deactivation, and mass transfer limitations may still be problems [1].

In order to avoid some of these disadvantages, the development of a vapour phase process is still in the focus of research. Expected advantages are simpler reactor technology, more convenient catalyst handling, and the avoidance of mass transfer limitations and solvent use. An overview of several currently investigated approaches to a vapour phase epoxidation of propene is given in [6–8]. One promising route utilises nitrous oxide (N_2O) as oxidant, which also led to a breakthrough in the highly selective hydroxylation of aromatic hydrocarbons, like benzene to phenol [9,10]. Duma and Hönicke were the first to investigate the catalytic propene epoxidation using silica supported iron oxide promoted with sodium ions. They obtained a maximum selectivity of 50% to propylene oxide at propene conversions of 5–10% at 648 K [11]. Our efforts in catalyst development led to a silica supported iron oxide system promoted with caesium-ions and -oxides ($CsO_x/FeO_y/SiO_2$), showing PO selectivities of 80% among the vapour phase products at similar propene conversions [7]. Recently, Wang

* Corresponding author. Tel.: +49 721 608 3947; fax: +49 721 608 6118.
E-mail address: andreas.reitzmann@ciw.uni-karlsruhe.de (A. Reitzmann).

0926-860X/$ – see front matter © 2006 Elsevier B.V. All rights reserved.
doi:10.1016/j.apcata.2006.10.051

Nomenclature

A	surface (m^2)
AA	allyl alcohol
c	molar concentration (mol m^{-3})
Ca	Carberry number (Eq. (3))
CTOR	catalytic total oxidation reactor
d_i	reactor inner diameter (m)
d_p	particle diameter (m)
D_{eff}	effective diffusion coefficient (m^2 s^{-1})
HMP	higher molecular weight products
k_{eff}	effective rate constant, based on volume (s^{-1})
k_m	rate constant, based on catalyst mass (m^3 kg^{-1} s^{-1})
l	reactor length (m)
m	mass (g)
$m_{cat.}$	catalyst mass (g)
m_C	mass of carbon (g)
$\tilde{M}$	molar mass (g mol^{-1})
n	amount of substance (mol)
$\dot{n}$	molar flow (mol s^{-1})
p	pressure (bar)
PA	propionaldehyde
PO	propylene oxide
$S_{i,r}$	selectivity of product i related to reactant r (Eq. (6))
t	time (s)
t_{mod}	modified residence time (kg_{cat} s m^{-3}, Eq. (1))
tos	time-on-stream (min)
T	temperature (K)
V	volume (m^3)
$\dot{V}$	volumetric flow (ml min^{-1})
Wz	Wheeler–Weisz modulus (Eq. (2))
x	molar fraction
X	conversion (Eq. (4))
X^*	normalised conversion (Eq. (5))

Greek symbols

α_i	carbon number of substance i
β	mass transfer coefficient (m s^{-1})

Subscripts

accum.	accumulation
AA	allyl alcohol
Acr.	acrolein
AC	acetone
b	bulk
BM	bypass mode
C	carbon
$C_3^=$	propene
HMP	higher molecular weight products
in	entering the system
out	leaving the system
p	particle
PA	propionaldehyde
PO	propylene oxide
r	reactant
RM	reactor mode
s	surface
TG	thermogravimetry

et al. reported even higher PO selectivities at conversions of 2–3% using SBA-15 and MCM-41 supported iron oxide and Fe-MFI zeolite, all promoted with potassium chloride [12–14]. The results of all mentioned studies have shown that alkaline metal salts and oxides are necessary for obtaining high PO selectivities. A strong deactivation was reported in all investigations, presumably due to coking of the catalyst. In contrast to other research groups, we have recently suggested that the carbon deposits on the catalysts must be considered as important byproducts in the carbon balance [15].

All research groups investigating the epoxidation of propene with N_2O over similar catalyst systems [7,11–14], did find mostly the same reaction products, namely propylene oxide, propionaldehyde, acetone, acrolein, allyl alcohol, CO, and CO_2. However, a meaningful comparison of the product spectra is hardly possible because Wang et al. [12–14], for example, lumped the side products PA, acetone, and acetaldehyde into one species. In addition, almost no information about proposed reaction paths is provided in the mentioned studies, because therein the residence time was not varied. Therefore, the present study focuses on the determination of the reaction network in the epoxidation of propene with N_2O. In particular, the effect of the formation of carbonaceous deposits was taken into account. The residence time was varied in a broad range, and propylene oxide and propionaldehyde were added to the reactor feed to determine the importance of different side reactions.

2. Experimental

2.1. Reaction unit and catalyst

A schematic view of the experimental set-up is given in Fig. 1. The catalytic measurements were carried out in an integral fixed bed reactor (stainless steel, $l = 300$ mm,

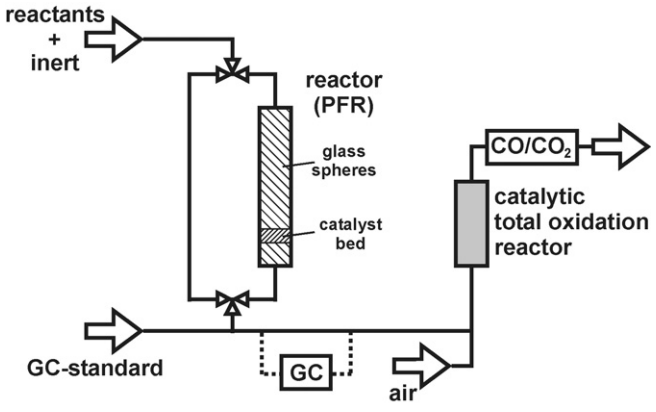

Fig. 1. Scheme of the reaction unit.

$d_i = 15$ mm) containing a silica supported iron oxide catalyst (1072 ppm mol/mol) promoted with caesium oxide (780 ppm mol/mol). The particle size fraction was 0.3–0.5 mm. The preparation of the catalyst is described in detail in [7]. The catalyst bed was diluted with glass spheres ($d_p = 0.5$ mm, volume ratio catalyst:glass = 2:1) to ensure isothermal conditions. This was proven through measuring the axial temperature profile with a thermocouple placed in the catalyst bed. Flow of reactants (propene 99.5% v/v, N_2O 99.995% v/v, PO 1.0% v/v in helium (99.995% v/v), PA 1.0% v/v in helium (99.995% v/v); Air Liquide) was adjusted with thermal mass flow controllers. Reactants and products were quantitatively analysed by means of gas chromatography (Varian CP 3800, equipped with a column PoraPlotQ and two detectors, TCD and FID) using an internal standard (propane 1.0% v/v in helium (99.995% v/v)). The unit allows for measurements in both, reactor and bypass mode. A catalytic total oxidation reactor downflow (catalyst: 1% w/w Pd on Al_2O_3) equipped with a non-dispersive infrared (NDIR) spectrometer (BINOS, Leybold–Heraeus) for CO and CO_2 detection was used for the on-line monitoring of the carbon balance.

In all catalytic measurements, pressure and temperature were kept at 1.3×10^5 Pa and 648 K, respectively. The modified residence time t_{mod}, defined as

$$t_{mod} = \frac{m_{cat}}{\dot{V}(T, p)}, \tag{1}$$

was varied between 100 and 2000 kg_{cat} s m^{-3} for propene conversion and between 10 and 220 kg_{cat} s m^{-3} for propylene oxide and propionaldehyde conversion.

The inlet concentrations of propene, PO, PA, and N_2O were varied in the range of 1–5% v/v, 0.1–0.3% v/v, 0.1–0.4% v/v, and 2–20% v/v, respectively. Helium (99.995% v/v; Air Liquide) was used as an inert diluent. In order to deduce the reaction network, only experiments with inlet concentrations of 1.0% v/v propene, 0.2% v/v PO, 0.2% v/v PA, and 15% v/v N_2O are used. It was found that the reactant feed concentration does not affect the reaction network. The effect of reactant concentration on the rates of individual reactions will be shown in a forthcoming publication.

Mass transfer effects both inside and outside the catalyst particle can be neglected for propene, propylene oxide, and propionaldehyde conversion. This is indicated by the small values obtained for Wheeler–Weisz modulus [16] and Carberry number [17](see Table 1), which are defined as

$$\mathrm{Wz} = \left(\frac{V_p}{A_p}\right)^2 \frac{k_{eff}}{D_{eff}}, \tag{2}$$

$$Ca = \frac{k_{eff}}{\beta(V_p/A_p)} = \frac{c_{i,bulk} - c_{i,surface}}{c_{i,bulk}}, \tag{3}$$

presuming first order rate laws. Therein k_{eff} denotes the effective rate constant, D_{eff} is the effective diffusion coefficient in the interior of a catalyst particle, and β is the mass transfer coefficient from the vapour phase to the particle outer surface.

Table 1
Characteristic numbers for estimation of mass transfer effects

Reactant	*Ca* [a]	Wz[b]
Propene	5.0×10^{-7}	5.1×10^{-6}
Propylene oxide	9.0×10^{-6}	1.0×10^{-4}
Propionaldehyde	7.7×10^{-6}	8.9×10^{-5}

[a] Carberry number [17].
[b] Wheeler–Weisz modulus [16].

2.2. Analysis of the experimental data

2.2.1. Conversion and selectivity

Conversion of a reactant was defined as

$$X = \frac{\dot{n}_{r,in} - \dot{n}_{r,out}}{\dot{n}_{r,in}}. \tag{4}$$

The molar flow of reactant entering ($\dot{n}_{r,in}$) and leaving ($\dot{n}_{r,out}$) the reactor was obtained by means of gas chromatographic analysis of the system effluent in bypass and reactor mode, respectively.

To compare the development of the catalyst activity over time-on-stream between different experimental runs, a normalised conversion was used related to the conversion after 70 min time-on-stream (tos):

$$X^*(\mathrm{tos}) = \frac{X(t = \mathrm{tos})}{X(t = 70\,\mathrm{min})}. \tag{5}$$

The selectivity was defined as the ratio of moles of product formed at the end of the reactor to the number of moles of the reactant that have been consumed, both multiplied with their carbon number α:

$$S_{i,r} = \frac{\alpha_i \dot{n}_i}{\alpha_r(\dot{n}_{r,0} - \dot{n}_r)}. \tag{6}$$

Plotting the selectivity of each product as function of the reactant's conversion is a valuable tool for evaluating the functional properties of the catalyst. Furthermore, if mass transport effects can be neglected, information on the reaction network can be gained from this plot [7,18,19]: the value obtained from extrapolating the selectivity trend of a certain product to zero conversion shows how this product is intrinsically formed. When the extrapolated selectivity differs from zero then the respective product is formed directly from the reactant, whereas if it equals zero then the product is formed via a consecutive pathway.

2.2.2. Carbon balance

The carbon balance is defined as

$$\dot{n}_{C,in} = \dot{n}_{C,out} + \dot{n}_{C,accum}. \tag{7}$$

The molar flow of carbon fed into the reactor is given by

$$\dot{n}_{C,in} = \alpha_r \dot{n}_{r,in}. \tag{8}$$

The experimental set-up (Fig. 1) provides the possibility to directly measure the molar flow of carbon entering the system. For that purpose, the feed stream ($\dot{n}_{feed}$) was not fed into the

reactor but through the bypass (BM = bypass mode) directly to the analytical set-up. An air flow ($\dot{n}_{air}$) was added to the feed stream and after the total oxidation reactor, the volumetric fraction of CO_2 ($x_{CO_2,BM}$) in the system effluent was measured using the NDIR spectrometer. Thus, the carbon feed stream can be calculated as

$$\dot{n}_{C,in} = (\dot{n}_{feed} + \dot{n}_{air}) x_{CO_2,BM}, \quad (9)$$

under the assumption of ideal gas behaviour.

Similarly, the flow of carbon leaving the reactor can be calculated in reactor mode (RM) as function of time:

$$\dot{n}_{C,out}(t) = \dot{n}_{out} x_{CO_2,RM}(t). \quad (10)$$

In bypass mode and during an experimental run, the feed and air flows were kept at the same constant level. The volume change caused by the reaction can be neglected due to the high surplus of inert gas. Thus, the combination of Eqs. (8)–(10) leads to

$$\dot{n}_{C,out}(t) = \frac{\alpha_r \dot{n}_{r,in}}{x_{CO_2,BM}} x_{CO_2,RM}(t). \quad (11)$$

The molar flow of carbon accumulating in the reactor can be derived from the combination of Eqs. (7), (9) and (11):

$$\dot{n}_{C,accum}(t) = \alpha_r \dot{n}_{r,in} \left(1 - \frac{x_{CO_2,RM}(t)}{x_{CO_2,BM}}\right). \quad (12)$$

Thus, the selectivity to coke at a certain time-on-stream (tos) can be calculated with

$$S_{C,r}(t = tos) = \frac{\dot{n}_{C,accum}(t = tos)}{(\alpha_r \dot{n}_{r,in} - \dot{n}_{r,out}(t = tos))}. \quad (13)$$

Multiplying of the integral of Eq. (12) with the molar mass of carbon leads to the mass of carbon accumulated inside the reactor after a certain time-on-stream (tos):

$$m_{C,accum}(t = tos) = \alpha_r \dot{n}_{r,in} \tilde{M}_C \int_0^{tos} \left(1 - \frac{x_{CO_2,RM}(t)}{x_{CO_2,BM}}\right) dt. \quad (14)$$

Additionally, the amount of carbonaceous species deposited on the catalyst was examined by means of thermogravimetry. The spent catalyst was placed in an air flow, whilst increasing the temperature from 293 to 1273 K at 2 K/min and the mass change was recorded (Netzsch STA 409). It was assumed that the deposits only consist of carbon.

The sum of selectivities obtained from the gas chromatographic analyses did never reach 100% (see Section 3.1). This was compensated by defining a species not detectable by means of gas chromatography designated as "higher molecular weight products" (HMP) that has a selectivity calculated with

$$S_{HMP,C_3^=} = 1 - \sum_i S_{i,C_3^=}. \quad (15)$$

3. Experimental results and discussion

3.1. Catalyst deactivation and carbon balance

Deactivation of the catalyst was observed in all experiments. Characteristic trends of this deactivation are shown in Fig. 2A for the applied reactants using the normalised conversion. These trends were found to be independent of the reactant concentrations and of the residence time. Hence, the same deactivation state of the catalyst at a given time-on-stream can be assumed and the kinetics can be regarded uncoupled from the deactivation kinetics.

Fig. 2A also shows that the catalyst deactivation was faster, when propene was used as reactant. Although the deactivation slows down after about 140 min, a steady-state conversion was

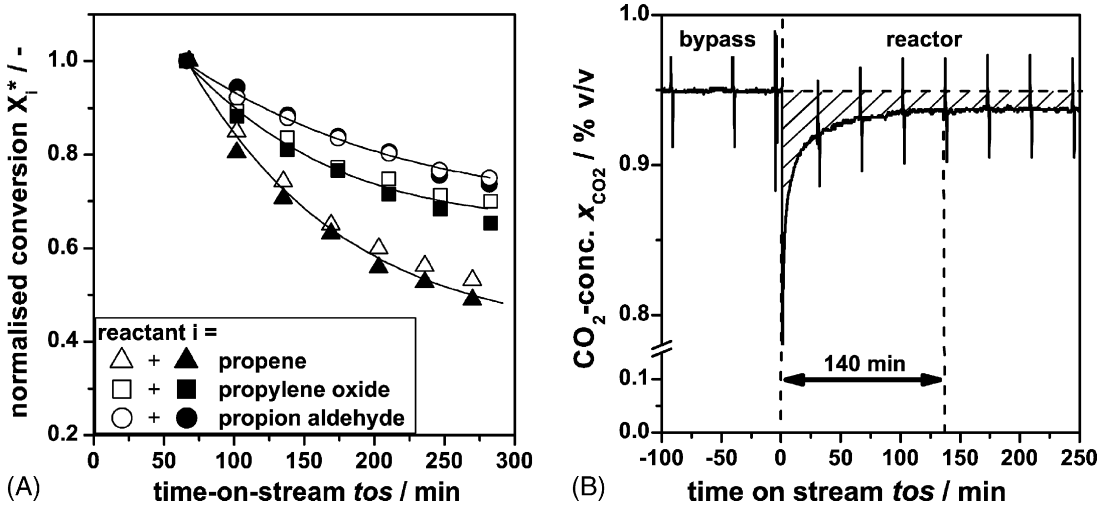

Fig. 2. (A) Catalyst deactivation: normalised conversion (Eq. (5)) for different reactants vs. time-on-stream. Exemplary trends at opposed reactant concentrations (open symbols: propene 1% v/v, PO 0.1% v/v, PA 0.1% v/v; filled symbols: propene 5% v/v, PO 0.4% v/v, PA 0.4% v/v; 15% v/v N_2O). (B) Carbon balance: trend of the CO_2 concentration in the effluent of the catalytic total oxidation reactor during an experimental run (peaks indicate the drawing of a sample for gas chromatography).

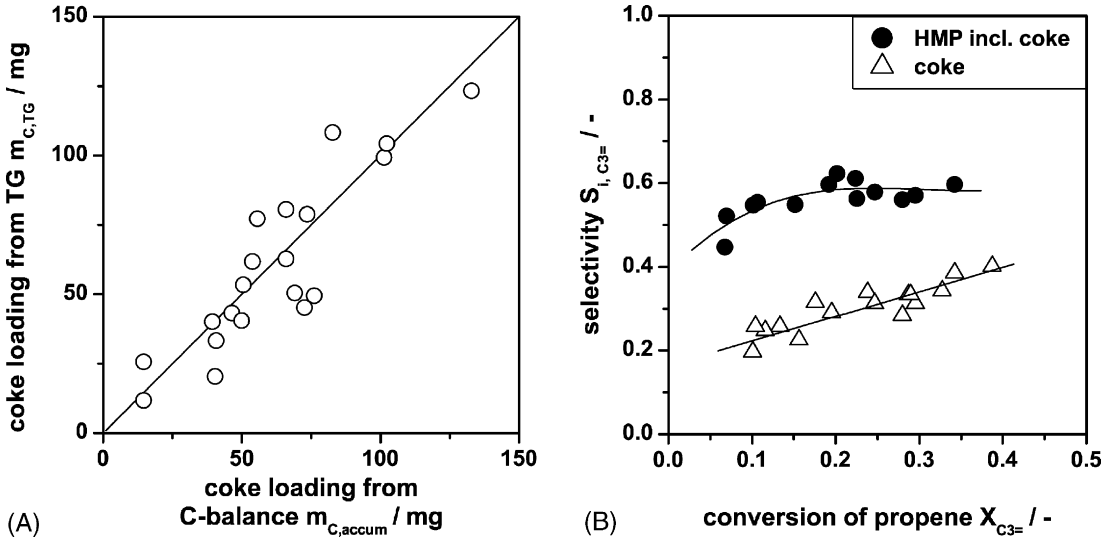

Fig. 3. (A) Methods for the estimation of the mass of coke deposits on the catalyst: parity plot of thermogravimetric (TG) analysis vs. on-line monitoring of the carbon balance (C-balance, Eq. (14)) and (B) selectivity to HMP determined by gas chromatography (filled circles, Eq. (15)) and coke obtained through monitoring the CO_2-concentration after the total oxidation reactor (blank triangles, Eq. (13)) vs. propene conversion ($x(C_3^=) = 1\%$ v/v, $x(N_2O) = 15\%$ v/v).

still not reached after 18 h time-on-stream with propene as a reactant (not shown). The reason for the deactivation is the formation of carbonaceous deposits (coke) on the catalyst surface. This becomes clear because of two reasons: firstly, the colour of the catalyst changed from white to black during operation and, secondly, the activity of a fresh sample can be restored by catalyst regeneration in air at temperatures of 773 K for 2 h. During regeneration, the coke species were burned off to CO_2 and H_2O.

Monitoring the carbon balance by means of measuring the CO_2 concentration after the catalytic total oxidation reactor (CTOR) was used as a tool to observe the formation of coke species during propene epoxidation (Fig. 2B): after switching from bypass to reactor mode, it took about 140 min until the CO_2 concentration was stationary but at that time only 90–95% of the CO_2 concentration measured in bypass mode was reached. The missing CO_2 can be correlated to the deficit in the carbon balance as shown in Section 2.2.2. The area between the CO_2 concentrations measured in bypass and reactor mode denotes the amount of carbon remaining inside the reactor (hatched area in Fig. 2B). Note that tracer measurements have shown that the reactor exhibits the response behaviour of a plug flow reactor. Thus, the residence time distribution can be neglected regarding the behaviour in Fig. 2B. In the following, steady-state conditions have been defined at 140 min (''pseudo-steady-state''), because the deficit in the carbon balance is constant after that time.

To validate the presented method, the coke on spent catalysts was burnt off by means of thermogravimetry. The results are shown as a parity plot in Fig. 3A and are consistent to a large extent for both methods. Thus, we can conclude that the shown on-line monitoring of the carbon balance in our set-up is a valuable method for the real time observation of the coke formation with high time resolution and accuracy.

In all experiments, the sum of selectivities to the reaction products obtained from the gas chromatographic analysis did never reach 100%. As solid products like coke cannot be detected by gas chromatography, at least a part of this deficit must be caused by coke. Fig. 3B shows the selectivity to coke as a function of propene conversion, calculated according to Eq. (13), compared to the selectivity to products not detectable in the GC calculated from Eq. (15), after a time-on-stream of 140 min. The comparison of both trends reveals that coke formation can only account for about half of the products not detectable in the GC. Thus, other high molecular products must be formed during the conversion of propene, PO, and PA. These products likely consist of higher alkenes and alkyl aromatics, but also high molecular oxygenates are possible, as found in the hydroxylation of benzene with N_2O [10,20,21]. In the following, carbonaceous deposits and unidentified products are merged in one chemical species designated as ''higher molecular weight products'' (HMP).

3.2. Product spectra and reaction network

A deep insight into the network of reactions proceeding during the epoxidation of propene using N_2O was gained by converting not only propene but also two of the major products: propylene oxide and propionaldehyde. Both substances were fed into the reactor under the same reaction conditions, but in the range of the low concentrations formed during propene epoxidation (0.1–0.4% v/v).

Table 2 shows the rate coefficients for the conversion of these reactants under the presumption of a first order rate law

Table 2
First order rate constants k_m for the conversion of propene, PO, and PA

Reactant	k_m ($m^3\ kg^{-1}\ s^{-1}$)
Propene	3.1×10^{-4}
Propylene oxide	5.6×10^{-3}
Propionaldehyde	9.6×10^{-3}

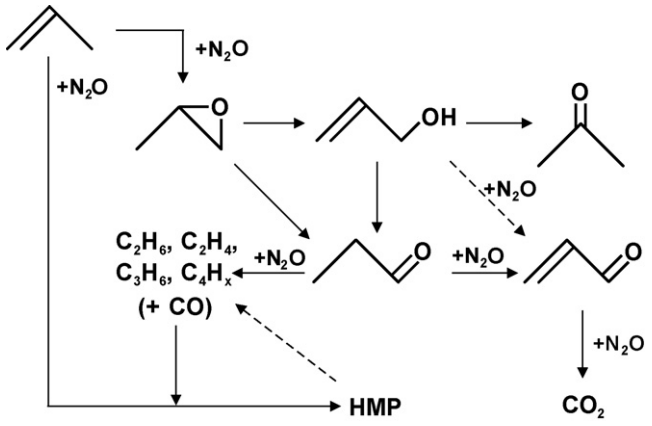

Fig. 4. Proposed reaction network of the catalytic propene epoxidation (stoichiometry was disregarded, HMP = higher molecular weight products).

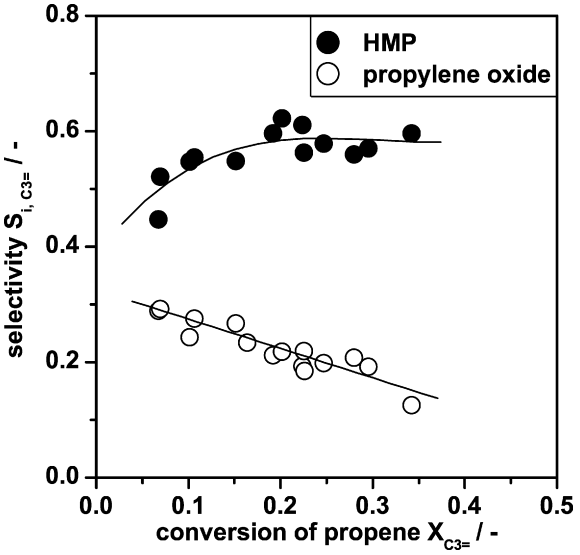

Fig. 5. Propene conversion: selectivity to propylene oxide and higher molecular weight products (HMP) vs. propene conversion ($x(C_3^=) = 1\%$ v/v, $x(N_2O) = 15\%$ v/v).

and ideal plug flow behaviour:

$$\frac{dc_r}{dt_{mod}} = -k_m c_r. \quad (16)$$

The estimated rate coefficients show that the products of propene conversion, PO and PA, are converted more than 10 times faster than propene itself. This displays that PO and PA are highly reactive intermediate products and that short residence times are necessary to obtain high PO selectivities.

From the obtained trends of the selectivities as functions of the conversions of propene, PO, and PA, the reaction network presented in Fig. 4 was revealed. Compared to the one presented before [7], some substantial modifications were made to comply with the latest experiments, particularly after converting PO and PA, and with respect to the previously introduced species HMP.

In the following, the reaction paths will be discussed in detail by means of interpreting the selectivity plots obtained from the conversion of propene, PO, and PA.

3.2.1. Propene conversion

The main products of propene conversion in the presence of N_2O were PO and HMP. Fig. 5 shows a selectivity plot for both substances. A steep decrease in selectivity to PO with increasing propene conversion was observed and the PO selectivity extrapolated to zero conversion was about 0.3–0.4. This indicates that PO is a primary product of propene conversion which is rapidly converted to consecutive products. In the same way, HMP can be identified as a primary product, but in contrast, selectivity to HMP increased with increasing propene conversion up to a limit of 60%.

Other products of propene conversion were propionaldehyde (PA), allyl alcohol (AA), acetone, light alkanes and alkenes (C_1, C_2, and C_4), and CO_2, as well as trace amounts of acrolein and acetaldehyde ($S \leq 1\%$, not shown). Selectivities to acetone, CO_2, and light alkanes and alkenes increased with propene conversion, while those to AA and PA pass a maximum at about 10% conversion before they decreased (Fig. 6). The selectivities of the

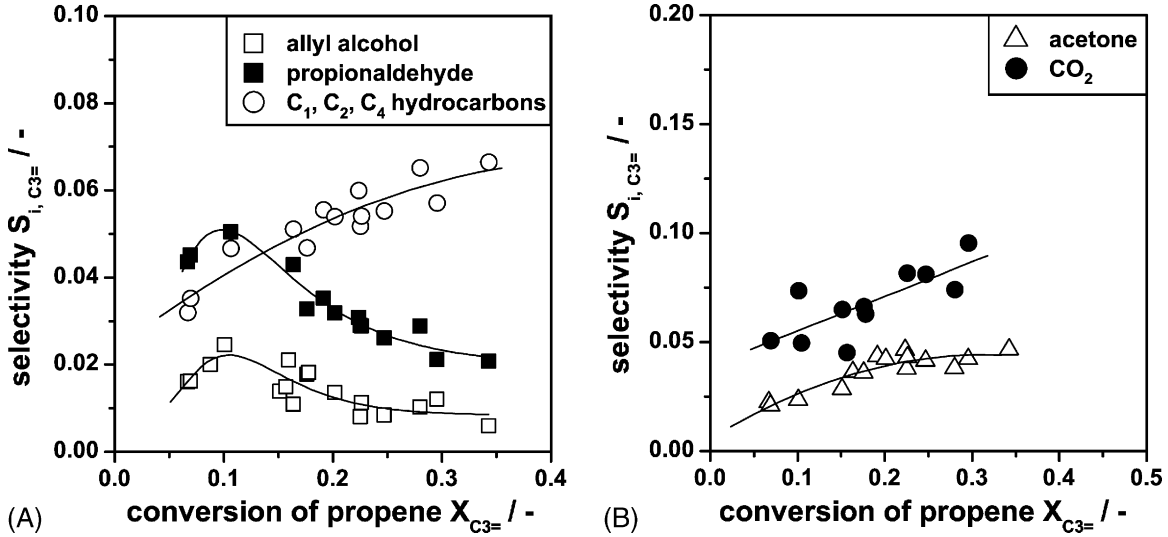

Fig. 6. Propene conversion: selectivity to (A) allyl alcohol, propionaldehyde, and light alkanes and alkenes and to (B) acetone and CO_2 vs. propene conversion ($x(C_3^=) = 1\%$ v/v, $x(N_2O) = 15\%$ Agreement v/v).

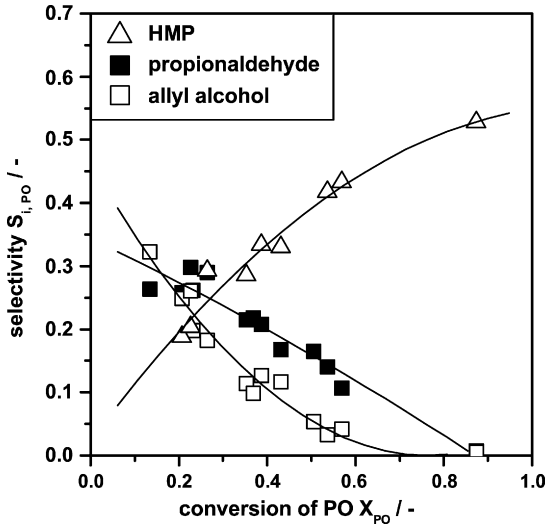

Fig. 7. PO conversion: selectivity to higher molecular weight products (HMP), propionaldehyde aldehyde, and allyl alcohol vs. PO conversion (x(PO) = 0.1–0.4% v/v, $x(N_2O)$ = 15% v/v).

latter products can be extrapolated to a selectivity of zero at zero conversion. This contradicts the suggestions in our previous work [7,15], but the extended experimental data obtained from investigations in the range of low propene conversions now clearly supports this trend. Hence, no direct formation pathway for PA and AA from propene is provided in the reaction network (Fig. 4). Both products are assumed to be formed through the fast isomerisation of PO, which is shown in Section 3.2.2. It seems to be reasonable to neglect a direct formation of acetone and light hydrocarbons from propene due to the very low values obtained by extrapolating their selectivity to zero conversion. In the case of CO_2, no clear proposition can be made due to the high variance of the CO_2 selectivities. However, a consecutive formation via oxygenates seems to be more likely than a direct formation.

3.2.2. *Propylene oxide conversion*

The conversion of PO mainly proceeded to AA, PA, and HMP, which is shown in the selectivity plot in Fig. 7. As the selectivities to AA and PA extrapolated to zero conversion reveal values of $\approx$0.5 and $\approx$0.35, respectively, it is clearly indicated that both products are formed directly through PO isomerisation. Both products are highly reactive intermediates shown by the steep decrease in selectivity down to zero with increasing PO conversion. In contrast, the selectivity to HMP increased with increasing PO conversion from 0 up to over 50%. Thus, HMP are formed as consecutive products.

Other products of PO conversion were CO_2, light alkanes and alkenes (C_1–C_4), acetone, acrolein, and acetaldehyde, all of them showing selectivities of zero at zero conversion (Fig. 8). Selectivities to all of these consecutive products, except acrolein and acetaldehyde, increased with increasing PO conversion over the investigated interval. The selectivity trends of acrolein and acetaldehyde both pass trough a maximum at around 30% conversion. Thus, among the consecutive products of PO conversion, only acrolein and acetaldehyde are further converted.

Studies on the influence of acid–base properties on the isomerisation of PO, like the ones conducted by Imanaka et al. [22–24], allow some statements about the active sites of our catalyst. It was reported that PA and acetone are produced on acidic and basic sites, respectively, whereas AA is formed on acid–base bifunctional sites. The comparison between their results and ours indicates that our catalyst still provides a high density of acid sites, although their strength must be quite low. This explains why no acetone is directly formed through isomerisation.

The results of Fási et al. [25], who studied the PO isomerisation over different catalysts, support our observations to some extent. The PO conversion over zeolites resulted in PA, acetone, and in dimers of PO, dependent on the type of zeolite. The dimers can be categorised into our HMP species. In contrast to our results, Fási et al. observed PA as a major product, even at PO conversions $\geq$60%. This difference is caused by the presence of N_2O in our investigation, which leads to a fast conversion of PA (see Table 2).

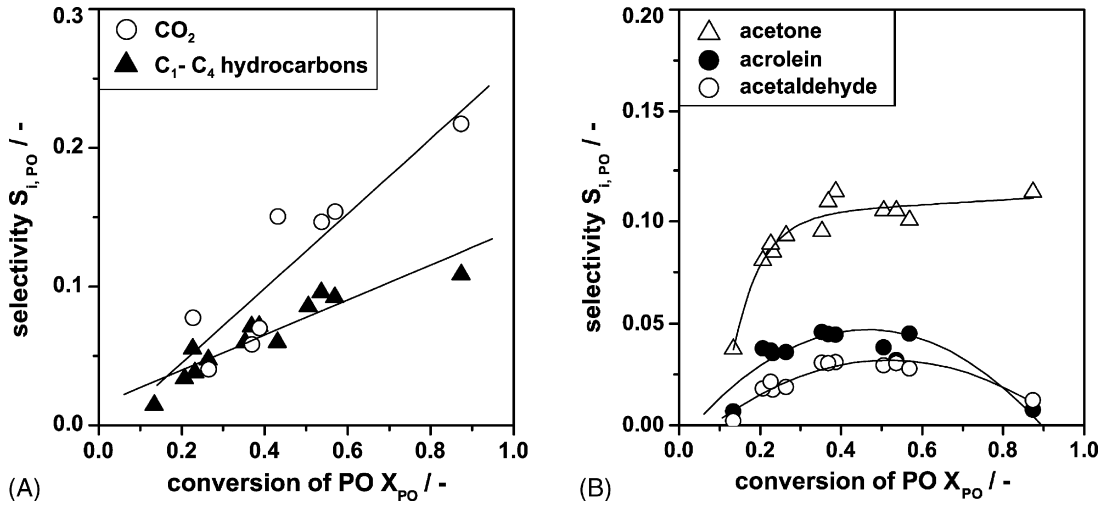

Fig. 8. PO conversion: selectivity to (A) CO_2 and light alkanes and alkenes, and to (B) acetone, acrolein, and acetaldehyde vs. PO conversion (x(PO) = 0.1–0.4% v/v, $x(N_2O)$ = 15% v/v).

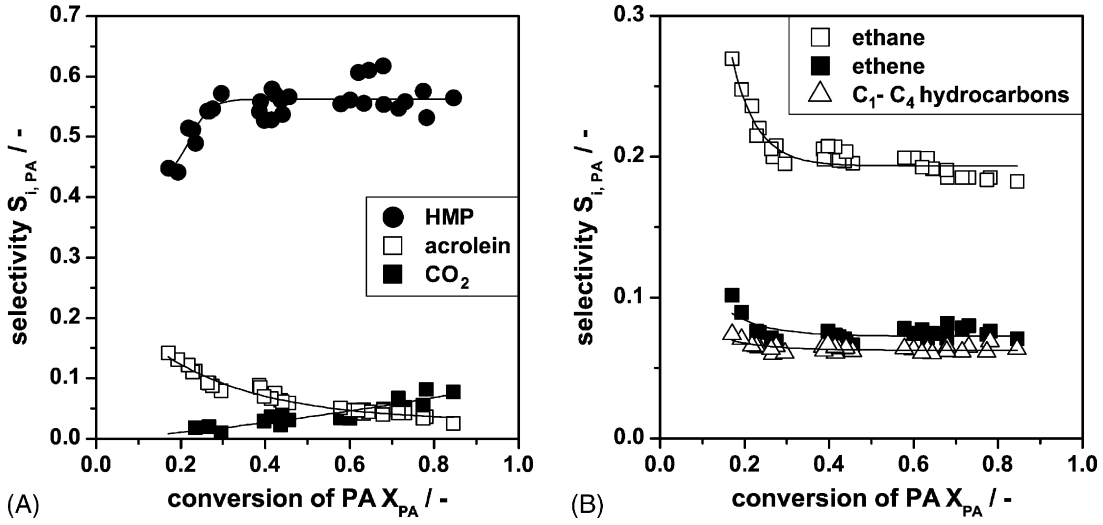

Fig. 9. PA conversion: selectivity to (A) higher molecular weight products (HMP), acrolein, and CO_2, and to (B) light alkanes and alkenes vs. PA conversion (x(PA) = 0.1–0.4% v/v, $x(N_2O)$ = 15% v/v).

Another possible product of PO isomerisation, methyl vinyl ether, which was observed in the homogeneous conversion of PO [26,27], was not found in the present study.

3.2.3. Propionaldehyde conversion

When PA was converted in the presence of N_2O, the main products were HMP, ethane, ethene, and acrolein. As shown in Fig. 9A, a steep increase in selectivity to HMP from 45 to 55% was observed between 15 and 30% conversion. The extrapolation of this trend to zero conversion results in a very low ($\leq$10%) selectivity to HMP. Thus, the consecutive formation of HMP is definitely faster than a primary formation from PA. As the selectivity to HMP reached a limit of 55–60% at PA conversions $\geq$30%, they seem to be not converted to consecutive products.

The selectivities to ethane and ethene steeply decreased with increasing conversion from 0.5 and 0.2 at zero conversion, respectively, until at 30% conversion constant selectivities of 0.2 and 0.08, respectively, were reached (Fig. 9B). A similar trend was observed for the other hydrocarbons (C_1, C_3, and C_4), but at lower selectivities. Thus, all the C_1–C_4 hydrocarbons seem to be formed as primary products. These species are assumed to be the result of cracking and oxidative C–C bond cleavage. The results of Ács et al. [28,29] support this idea. They also observed ethane as major product, ethene and methane in lower concentrations and propene and butane in traces in the homogeneous PA decomposition. When PA is decomposed to ethene, CO should remain, which was detected as major product by Ács et al. In our investigations, CO was also observed, but could not be quantified due to current analysis constraints.

Due to the complementary selectivity trends of (a) HMP and (b) ethane, ethene, and other hydrocarbons, we can conclude that HMP are formed at least partially from the latter. The fact that both substance classes reach a stationary selectivity at PA conversions higher than 30% allows the assumption that the reaction from C_1–C_4 hydrocarbons to HMP can also run in the opposite direction. This means that on acidic surface sites both HMP cracking and formation take place.

The selectivity to acrolein extrapolated to zero conversion was 0.25–0.3. As shown in Fig. 9A, the selectivity to acrolein decreased with increasing PA conversion. Thus, acrolein is formed directly from PA through oxidative dehydrogenation with N_2O and is fast converted to consecutive products. As the selectivity to CO_2 increased with increasing PA conversion, starting from a selectivity of zero (Fig. 9A), which is complementary to the trend of acrolein selectivity, it is most likely that CO_2 is one of the products acrolein is directly converted to.

Further products of PA conversion in the presence of N_2O were traces of allyl alcohol (S = 1.5%), and acetaldehyde (S = 1%). Note that no acetone was formed in the PA conversion. Since acetone is no primary product of propene and PO conversion (Figs. 6B and 8), we assume that it is formed through the conversion of AA. This seems to be reasonable because AA was identified as a highly reactive intermediate product. Acetone is assumed to be unreacted under the investigated reaction conditions, as its selectivity was increasing with increasing conversion of both PO and propene (see Section 3.2.1).

During the experiments, it was discovered that the concentration of N_2O has a great influence on the conversion of PA. The kinetic relevance of N_2O will be presented and discussed in a companion paper. In the complete absence of N_2O, however, only one single product could be detected by gas chromatography besides traces of allyl alcohol. This product could not be clearly identified but due to its retention time, it is believed that this substance is a dimer of propionaldehyde. On the basis of this assumption, a relative molar response factor between 420 and 450 can be estimated according to Ackman [30]. This would lead to a selectivity of approximately 65–75% at a PA conversion of 26%. This oxygen containing dimer could be a highly reactive precursor for the products of cracking reactions. In the presence of N_2O, the formation of these

species is either prevented or, more likely, these species are quickly converted to the cracking products mentioned above. The possible formation of such products was also reported in [25], but for the direct PO isomerisation. We already assumed these kinds of species as intermediates before [7], but we are still not able to analyse and quantify them exactly.

The product of complete oxidation, CO_2, is not primarily formed when converting propene, PO, and PA, because in each case the selectivity extrapolated to zero conversion equals zero (Figs. 6B, 8A and 9A). Thus, the pathway of CO_2 formation is still unknown. One possible source could be the combustion of acrolein or allyl alcohol because they seem to be the only substances that undergo a quick subsequent conversion (Figs. 7, 8B and 9A).

4. Conclusions

The vapour phase epoxidation of propene with nitrous oxide (N_2O) as an oxidant was investigated in a fixed bed reactor in a broad range of residence times. A silica supported iron oxide catalyst promoted with caesium oxides/ions was used.

Allyl alcohol and acrolein were found only in traces when converting propene. According to Duma and Hönicke [11], the conclusion from these results is that the applied catalyst strongly favours the path of vinylic oxidation to PO as compared to the path of allylic oxidation. However, our results show that allylic alcohol and acrolein in the product spectra are not necessarily an indicator for the existence of the allylic oxidation pathway, because allyl alcohol is a product of PO isomerisation and acrolein is formed through oxidative dehydrogenation of PA.

The epoxidation reaction proceeds in a complex reaction network. This was revealed by the trends of the selectivities as functions of the conversions of propene, PO, and PA. Important side reactions are the PO isomerisation and the formation of high molecular weight products (HMP).

Although HMP cannot be exactly specified at the moment, we can distinguish between two species: carbonaceous deposits (coke) on the catalyst surface and other high molecular weight products in the vapour phase. Coke is assumed to be mainly formed from the reactant propene and other light alkanes and alkenes formed as cracking products of PA conversion. Coking is held responsible for the catalyst deactivation. Other HMP must be formed as primary or consecutive products during the conversion of propene, PO, and PA. These products likely consist of higher alkenes, alkyl aromatics, and higher oxygenates.

When HMP in general are regarded as products of the propene epoxidation, the PO selectivity is decreased by more than half compared to when only substances detected in the GC are taken into account. This fact is responsible for the discrepancy between the presented selectivities and our previous results using the same catalyst [7]. The formation of HMP was also not reported by other research groups [11–14] and therefore not taken into account for the calculation of conversion and/or selectivities. This seems inconsistent as other research groups consider carbonaceous deposits as responsible for catalyst deactivation. Note, that neglecting the significant formation of HMP makes it impossible to correctly determine the conversion of propene via the concentrations of the products detected by GC analysis and the remaining propene, like it is reported in [14], because then not all products are considered. Consequently, it is not possible to determine correct product selectivities with this method.

It was shown that catalyst deactivation by coking and the formation of higher molecular weight products are the main problems of this propene epoxidation route. Thus, further development of the catalyst should concentrate on the tuning of the acid–base properties, which will directly influence the consecutive conversion of PO, rather than the activation of N_2O and the generation of an appropriate oxygen species. Then, not only higher PO selectivities can be obtained, but also the long term stability of the catalyst can be improved.

The experimental data and the derived reaction network were used for the development and comparison of formal kinetic models for simulating the behaviour of an epoxidation reactor, which will be presented in a companion paper.

Acknowledgements

A. Reitzmann gratefully acknowledges financial support from Fonds der Chemischen Industrie (FCI), Germany. A. Wix would like to thank General Electric for granting the Edison Award. The authors thank Ryan Anderson from Bucknell University in Lewisburg, PA for editing and discussing the paper.

References

[1] Th. Haas, W. Hofen, G. Thiele, P. Kampeis, in: Proceedings of the DGMK-Conference 2001-4, Hamburg, Germany, (2001), p. 127.
[2] P. Arpentinier, F. Cavarni, F. Trifiro, The Technology of Catalytic Oxidations, vol. 1, TECHNIP, 2001, p. 231.
[3] M. McCoy, Chem. Eng. News 79 (2001) 19.
[4] M. Clerici, P. Ingallina, Catal. Today 41 (1998) 351.
[5] C. Perego, A. Carati, P. Ingallina, M.A. Mantegazza, G. Belussi, Appl. Catal. A 221 (2001) 63.
[6] J.R. Monnier, Appl. Catal. A 221 (2001) 73.
[7] E. Ananieva, A. Reitzmann, Chem. Eng. Sci. 59 (2004) 5509.
[8] T.A. Nijhuis, M. Makkee, J.A. Moulijn, B.M. Weckhuysen, Ind. Eng. Chem. Res. 45 (2006) 3447.
[9] G.I. Panov, CATTECH 4 (2000) 18.
[10] A. Reitzmann, E. Klemm, G. Emig, Chem. Eng. J. 90 (2002) 149.
[11] V. Duma, D. Hönicke, J. Catal. 191 (2000) 93.
[12] X. Wang, Q. Zhang, Q. Guo, Y. Lou, Y. Yang, Y. Wang, Chem. Commun. (2004) 1396.
[13] X. Wang, Q. Zhang, S. Yang, Y. Wang, J. Phys. Chem. B 109 (2005) 23500.
[14] Q. Zhang, Q. Guo, X. Wang, T. Shishido, Y. Wang, J. Catal. 239 (2006) 105.
[15] A. Reitzmann, T. Thömmes, A. Wix, B. Kraushaar-Czarnetzki, in: Proceedings of the DGMK-Conference 2005-2, Milan, Italy, (2005), p. 231.
[16] P.B. Weisz, Z. Phys. Chem. 11 (1957) 1.
[17] J.J. Carberry, in: J.R. Anderson, M. Boudard (Eds.), Catalysis: Science and Technology, vol. 8, Springer-Verlag, Berlin, 1987, p. 131.
[18] L. Riekert, Appl. Catal. 15 (1985) 89.
[19] H.G. Lintz, Oil Gas Sci. Technol. 57 (2002) 653.
[20] R. Burch, C. Howitt, Appl. Catal. A 106 (1993) 167.

[21] S. Perathoner, F. Pino, G. Centi, G. Giordano, A. Katovic, J.B. Nagy, Top. Catal. 23 (2003) 125.
[22] T. Imanaka, Y. Okamoto, S. Teranishi, Bull. Chem. Soc. Jpn. 45 (1972) 1353.
[23] T. Imanaka, Y. Okamoto, S. Teranishi, Bull. Chem. Soc. Jpn. 45 (1972) 3251.
[24] Y. Okamoto, T. Imanaka, S. Teranishi, Bull. Chem. Soc. Jpn. 46 (1973) 4.
[25] A. Fási, A. Gömöry, I. Pálinkó, I. Kiricsi, J. Catal. 200 (2001) 340.
[26] M. Flowers, J. Chem. Soc. 73 (1977) 1927.
[27] F. Dubnikova, A. Lifshitz, J. Phys. Chem. A 104 (2000) 4489.
[28] G. Ács, G. Tóth, P. Huhn, Acta Chim. (Budapest) 82 (1974) 317.
[29] G. Tóth, G. Ács, P. Huhn, Acta Chim. (Budapest) 82 (1974) 333.
[30] R.G. Ackman, J. Gas Chromatogr. 2 (1964) 173.